


Title: **Single-Step Formation of a Low Work Function Cathode Interlayer and n-type Bulk Doping from Semiconducting Polymer/ Polyethylenimine Blend Solution** 

Author(s): Keli Fabiana Seidel, Dominique Lungwitz, Andreas Opitz, Thomas Krüger, Jan Behrends, Seth R. Marder, and Norbert Koch

Document type: Preprint

Terms of Use: Copyright applies. A non-exclusive, non-transferable and limited right to use is granted. This document is intended solely for personal, non-commercial use.

Citation:

"ACS Appl. Mater. Interfaces 2020, 12, 25, 28801–28807 ; <https://doi.org/10.1021/acsami.0c05857>"

Single-step formation of low work function cathode interlayer and n-type bulk doping from semiconducting polymer/polyethylenimine blend solution

Keli Fabiana Seidel,^{1,2,*} Dominique Lungwitz,^{2,*} Andreas Opitz,^{2,*} Thomas Krüger,³ Jan Behrends,³ Seth R. Marder,⁴ and Norbert Koch^{2,5}

- ¹⁾ Physics Department, Universidade Tecnológica Federal do Paraná, Brazil
- ²⁾ Institut für Physik & IRIS Adlershof, Humboldt Universität zu Berlin, Germany
- ³⁾ Berlin Joint EPR Lab and Institut für Experimentalphysik, Freie Universität Berlin, Germany
- ⁴⁾ School of Chemistry and Biochemistry and Center for Organic Photonics and Electronics (COPE), Georgia Institute of Technology Atlanta, USA
- ⁵⁾ Helmholtz-Zentrum Berlin für Materialien und Energie GmbH, Germany

* These authors contributed equally.

Abstract

The use of polyethylenimine (PEI) as thin interlayer between cathodes and organic semiconductors in order to reduce interfacial ohmic losses has become an important approach in organic electronics. It has also been shown that such interlayers can form spontaneously due to vertical phase separation when spin coating a blended solution of PEI and the semiconductor. Furthermore, bulk doping of semiconducting polymers by PEI has been claimed. However, to our knowledge a clear delineation of interfacial from bulk effects has not been published. Here, we report a study on thin films formed by spin coating blended solutions of PEI and poly[N,N'-bis(2-octyldodecyl)naphthalene-1,4,5,8-bis(dicarboximide)-2,6-diyl]-alt-5,5'-(2,2'-bithiophene) [P(NDI2OD-T₂)] on indium-tin-oxide. We observed that vertical phase separation in such films, where PEI accumulates at the bottom and the top, sandwiching the semiconductor layer. The PEI interlayer on ITO reduces the electron injection barrier to the minimum value determined by Fermi level pinning, which, in turn, reduces the contact resistance by five orders-of-magnitude. While we find no evidence for doping-induced polarons in P(NDI2OD-T₂) upon mixing with PEI from optical absorption, more sensitive electron paramagnetic resonance measurements provide evidence for doping and an increased carrier density, at very low level. This, in conjunction with an increased charge carrier mobility due to trap filling, result in an increase of the mixed polymer conductivity by four orders-of-magnitude relative to pure P(NDI2OD-T₂). Consequently, both interfacial and bulk effects occur with notable magnitude in thin films formed from blended semiconductor polymer/PEI solution. Thus, this facile one-step procedure to form PEI interlayers must be applied with attention, as modification of the bulk semiconductor polymer (here doping) may occur simultaneously, and might go unnoticed if not examined carefully.

Introduction

Thin layers of polyethylenimine (PEI) and ethoxylated PEI (PEIE) are frequently applied to reduce the work function of a wide range of electrode materials, such as the conductive polymer mixture poly(3,4-ethylenedioxythiophene):polystyrene sulfonate, indium-tin oxide, zinc oxide, and graphite.[1–5] A preferential orientation of the amine groups' electric dipole at the interface was invoked to explain that work function reduction.[1] The lowered work function results in a reduced energy barrier for electrons between that electrode and a semiconductor, resulting in improved device performance. This includes all-polymeric solar cells [1,6], inverted organic photovoltaic cells [7–11], organic light emitting diodes [12–14], and perovskite solar cells [15,16]. In contrast, for films prepared from a blend solution of PEI and the n-type poly[N,N'-bis(2-octyldodecyl)naphthalene-1,4,5,8-bis(dicarboximide)-2,6-diyl]-alt-5,5'-(2,2'-bithiophene) [P(NDI2OD-T₂)], higher currents in field-effect transistors were observed compared to pristine P(NDI2OD-T₂) alone, which was ascribed to n-type doping of the semiconductor polymer by PEI.[17] An increased charge carrier mobility was proposed to result from doping in films prepared from blend solution. Solutions of PEI blended with semiconducting polymers and fullerene derivatives were also employed to form the active layers in bulk heterojunction solar cells.[18,19] Here, vertical phase separation and accumulation of PEI at interfaces was given as reason for improved device performance, due to a reduced electron injection barrier between electrode and the fullerene derivative, but doping of the semiconductor polymer was not identified.

In this study, we investigate the impact of blending of P(NDI2OD-T₂) with PEI in solution on charge carrier transport and morphology of corresponding thin films. Experiments are designed to allow a differentiation between modified energy level alignment at the electrical contact and effects due to doping. We find evidence for vertical phase separation that occurs during spin coating. A PEI interlayer forms between electrode and P(NDI2OD-T₂), reducing the contact resistance by about five orders-of-magnitude. Moreover, the semiconductor polymer conductivity increases by four orders-of-magnitude. In part, this is due to a minute level of doping of P(NDI2OD-T₂) by PEI, as we find the density of charge carriers only increasing by less than two orders-of-magnitude. As we find no apparent changes of the P(NDI2OD-T₂) morphology with and without PEI, we conclude that trap-filling due to doping enhances the charge carrier mobility significantly. The PEI-blended solution thus facilitates an easy and one-step deposition process for P(NDI2OD-T₂) thin films that results in two beneficial effects, i.e., reduced contact resistance and enhanced carrier mobility.

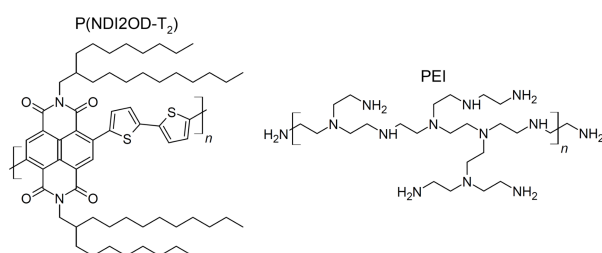


Figure 1. Chemical structure of poly[N,N'-bis(2-octyldodecyl)naphthalene-1,4,5,8-bis(dicarboximide)-2,6-diyl]-alt-5,5'-(2,2'-bithiophene) [P(NDI2OD-T₂)] and polyethylenimine (PEI).

Experimental details

Poly[N,N'-bis(2-octyldodecyl)naphthalene-1,4,5,8-bis(dicarboximide)-2,6-diyl]-alt-5,5'-(2,2'-bithiophene) [P(NDI2OD-T₂)] was purchased from Ossila, polyethylenimine (PEI, as powder) from Sigma-Aldrich. Figure 1 depicts the respective chemical structures. Two separate chloroform solutions of P(NDI2OD-T₂) and PEI with 5 mg/ml each were prepared. The blended solutions were prepared with the following P(NDI2OD-T₂):PEI mass ratios (monomer ratios): 98%:2% (95%:5%), 95%:5% (90%:10%)

and 90%:10% (82%:18%). P(NDI2OD-T₂):PEI blended solutions were stirred for 30 min prior to the deposition. Films were deposited by dynamic spin coating, i.e., deposited volume of 50 µl at 400 rpm for 5 s, film drying at 3000 rpm for 55 s. All steps were performed in inert nitrogen atmosphere.

For electrical characterization in two-terminal planar configuration, thin films were prepared on interdigitated indium-tin-oxide electrodes (on glass) purchased from Ossila (total channel width $w = 30$ mm, channel length / electrode distance $L = 50$ µm, or as specified in the text). The ITO had a thickness of 100 nm and a sheet resistance of 20 Ω/square. These substrates were cleaned by a sequence of acetone, isopropanol, and de-ionized water in an ultrasonic bath for 12 min in each step. Afterwards, the substrates were treated for 15 min in an UV Ozone Cleaner (Ossila). Immediately after this cleaning sequence, the polymer films were spin coated in inert nitrogen atmosphere. Current vs. voltage (I - V) curves were measured in inert nitrogen atmosphere with a Keithley 2635A source meter. The total resistance of the two-terminal devices was determined from recorded I - V curve from the slope as in

$$R_{total} = \frac{\partial V}{\partial I}. \quad (1)$$

To separate contact and channel resistance, the transfer length method was applied,[20] with channel lengths ranging from 50 µm to 200 µm. The channel resistance $R_{channel}$ depends linearly on L and the contact resistance $R_{contact}$ is independent of L in the analyzed channel length range. In this linear regime, the total resistance R_{total} is a function of L :

$$R_{total}(L) = R_{contact} + R_{channel}(L) = R_{contact} + \frac{L}{S}, \quad (2)$$

where S is the inverse slope of the R - L curve. The electrical conductivity of the polymer film σ is calculated from the slope S using the channel cross section (film thickness $d \times$ electrode width w) via

$$\sigma = \frac{S}{w \cdot d}. \quad (3)$$

The film morphology was characterized with a Bruker Dimension Icon scanning force microscopy, operated in peak force mode. Photoelectron spectroscopy measurements were performed with excitation from a He-discharge lamp (HeI, excitation energy 21.1 eV) and from Al K α X-ray source (excitation energy 1486.6 eV). Photoelectron spectra were recorded with a hemispherical analyzer (EA125, Omicron). The sample work function was determined by measuring the secondary electron cutoff, with the samples biased with -10 V to clear the analyzer work function. UV-vis-NIR absorption spectra were recorded with a Perkin Elmer Lambda 950, for solutions within a quartz glass cuvette (concentration kept at 0.225 mg/ml), and for films on quartz glass substrates, in ambient air and, for comparison, in inert nitrogen atmosphere; no differences were observed.

Samples for electron paramagnetic resonance (EPR) measurements were prepared by filling 50 µl of the polymer solutions into quartz tubes (inner diameter: 3 mm, outer diameter 3.9 mm) and then evaporating the solvent under vacuum, resulting in a solid film on the inner wall of the EPR tube. The EPR tubes were then backfilled with helium and flame-sealed using a blowtorch. X-band continuous wave EPR measurements were performed using a Bruker ER 4122 SHQE resonator in a laboratory-built spectrometer consisting of a Bruker ER 041 MR microwave bridge with an ER 048 R microwave controller, an AEG electromagnet with a Bruker BH15 Hall effect field controller and using a Stanford Research SR810 lock-in amplifier in combination with a Wangine WPA-120 modulation amplifier for field modulation and lock-in detection. The spectra were acquired at a microwave frequency of 9.389 GHz and a microwave power of 50 µW with a 100 kHz modulation frequency and 0.2 mT modulation amplitude. The background correction was performed with the spectrum recorded for an empty EPR tube inside the resonator cavity. The quality factor of the resonator was determined from the mode picture for each measurement and used for quantitative (spin counting) analysis. The

absolute number of unpaired electron spins in each sample was determined as described previously.[21]

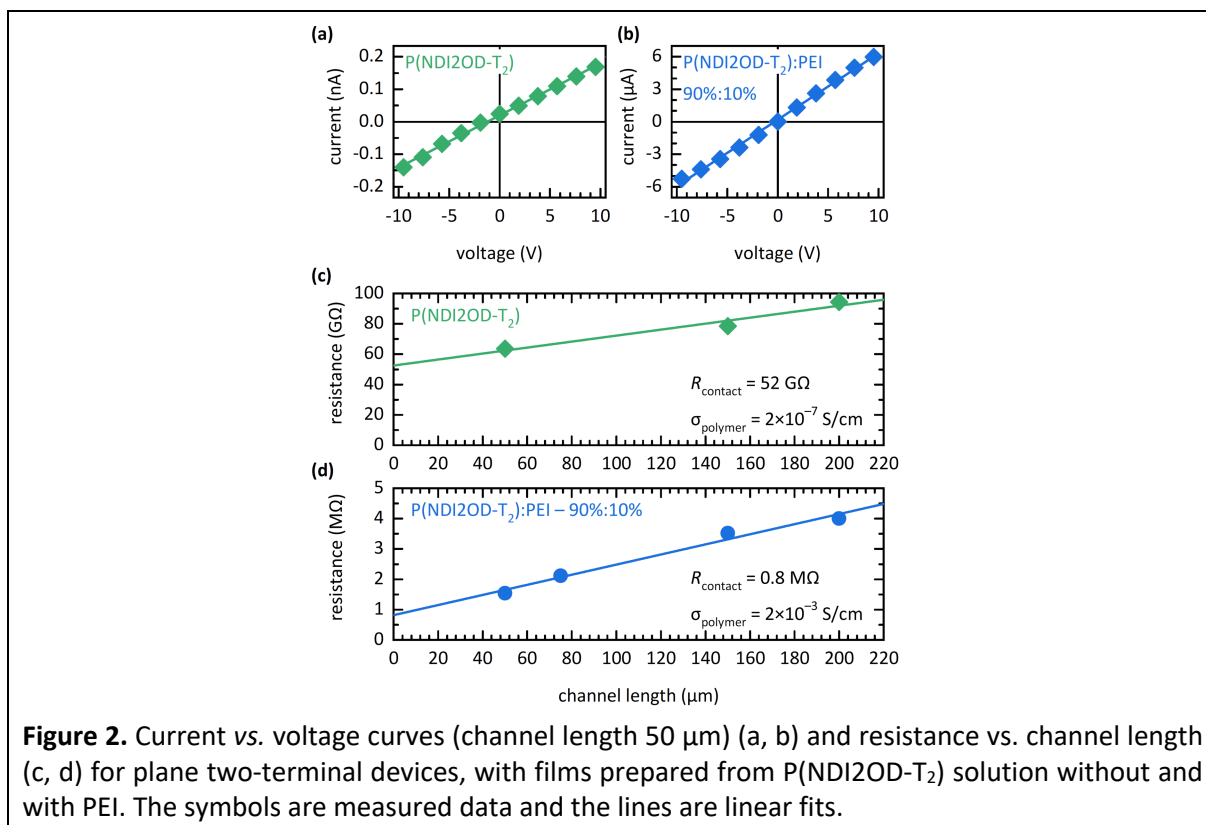
Results and discussion

The total resistance R_{total} measured for the two-terminal devices is given in Table 1. The resistance of a device containing a pure PEI film was higher than the detection limit of our setup, which is close to the resistance measured for the pure P(NDI2OD-T₂) film. Upon blending PEI in solution, R_{total} is reduced by about five orders-of-magnitude. Current-voltage curves are given exemplary for a pure P(NDI2OD-T₂) film and one made from P(NDI2OD-T₂):PEI (90%:10%) blend solution, exhibiting linearity of I and V . (Figure 2a, b). The current offset at the origin of the plot in Figure 2a gives an estimate of the uncertainty of the measurement, and it is in the range of the detection limit of the used setup.

Table 1. Total resistance R_{total} determined from I - V measurements on two-terminal devices (channel length 50 μm) for P(NDI2OD-T₂) without and with PEI blended in solution. The conductivity σ determined from the transfer length method is given for two samples. For blend solution the respective mass ratios are given.

R_{total} from two-terminal devices (Ω)	
pristine P(NDI2OD-T ₂)	3×10^{11}
from blend solution P(NDI2OD-T ₂):PEI – 98%:2%	3×10^6
from blend solution P(NDI2OD-T ₂):PEI – 95%:5%	1×10^6
from blend solution P(NDI2OD-T ₂):PEI – 90%:10%	1×10^6
thin film σ from transfer length method ($\text{S}\cdot\text{cm}^{-1}$)	
pristine P(NDI2OD-T ₂)	2×10^{-7}
from blend solution P(NDI2OD-T ₂):PEI – 90%:10%	2×10^{-3}

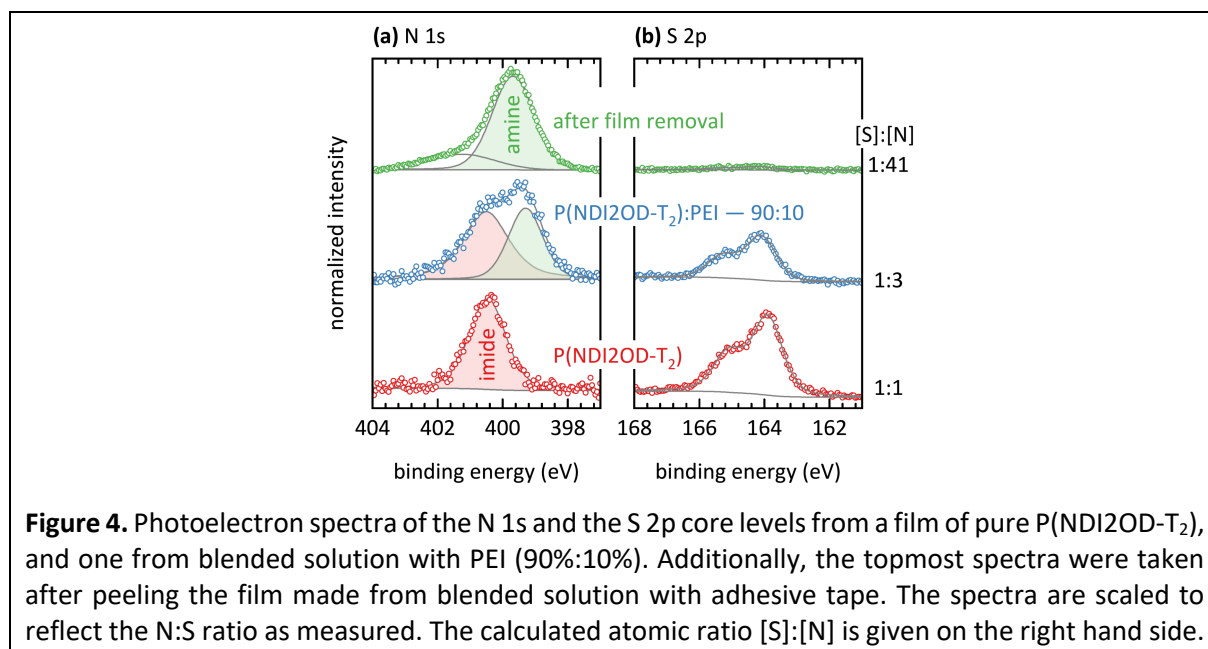
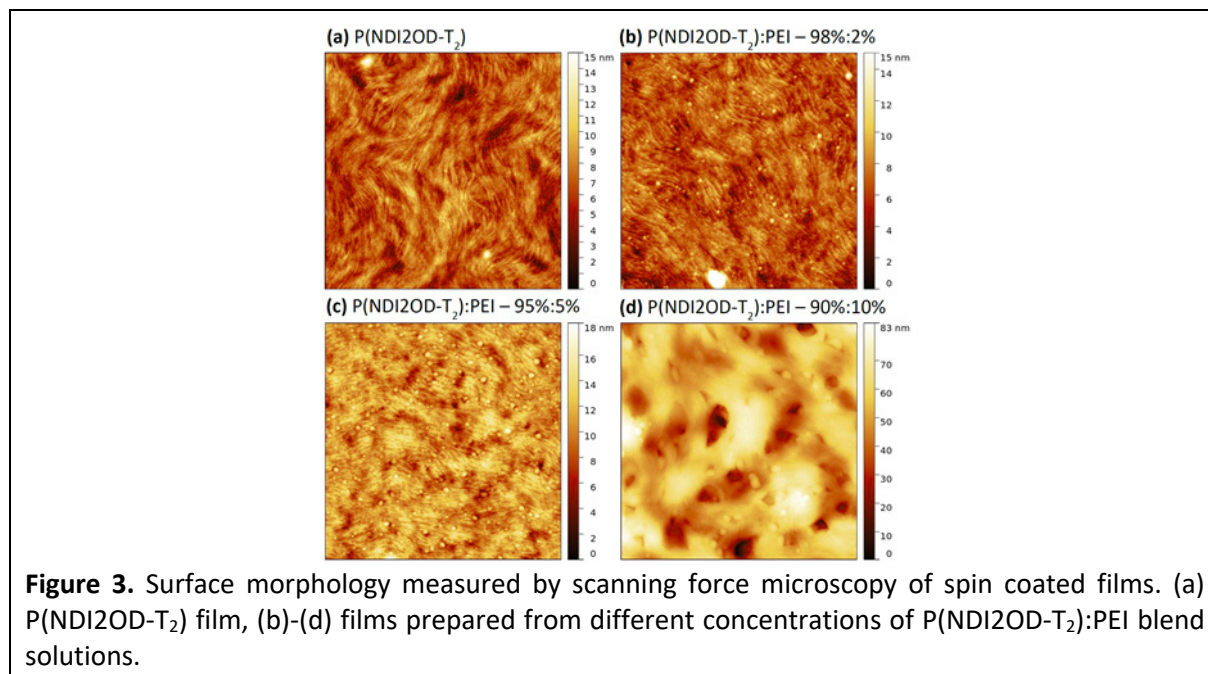
To differentiate contact and channel resistance, the transfer length method was applied to devices with a P(NDI2OD-T₂) film and a film prepared from P(NDI2OD-T₂):PEI (90%:10%) blend solution. The resistance vs. channel length curves are shown in Figure 2c and d. The contact resistance decreases by about five orders-of-magnitude, from 52 G Ω to 0.8 M Ω . In turn, the polymer film conductivity increases by four orders-of-magnitude, from $2 \cdot 10^{-7}$ S/cm to $2 \cdot 10^{-3}$ S/cm. Consequently, both contact resistance and channel conductivity are substantially affected by adding PEI in solution. The reduced contact resistance is a signature for reduced electron injection barrier. The increased channel conductivity might be related to different film morphology and/or increased charge carrier density due to doping.



First, we turn towards film morphology as characterized by scanning force microscopy (Figure 3). Typical fibrillae are observed for pure P(NDI2OD-T₂) films, as reported before.[22] These fibrillae are preserved upon adding 2% and 5% of PEI to the semiconductor polymer solution, but now also small dot-like features (bright spots) are observed, more of them for 5% PEI compared to 2%. Adding 10% of PEI in solution results in a film where the fibrillae are barely discernable (best in the darker, i.e., lower, areas). Instead, large-area carpet-like features cover most of the surface. Phase separation is known to occur in films spin-coated from two-polymers solution, where the interaction between the two polymers is very weak.[23]. In addition to the expected accumulation of PEI at the bottom of thin films, as discussed in the introduction above, precipitation of PEI also at the film surface seems plausible from our morphological observations. At the two lower PEI contents in the form of the dot-like features, and at 10% PEI in a comparably closed layer, as already observed for other blends of semiconducting and insulating polymers.[24]

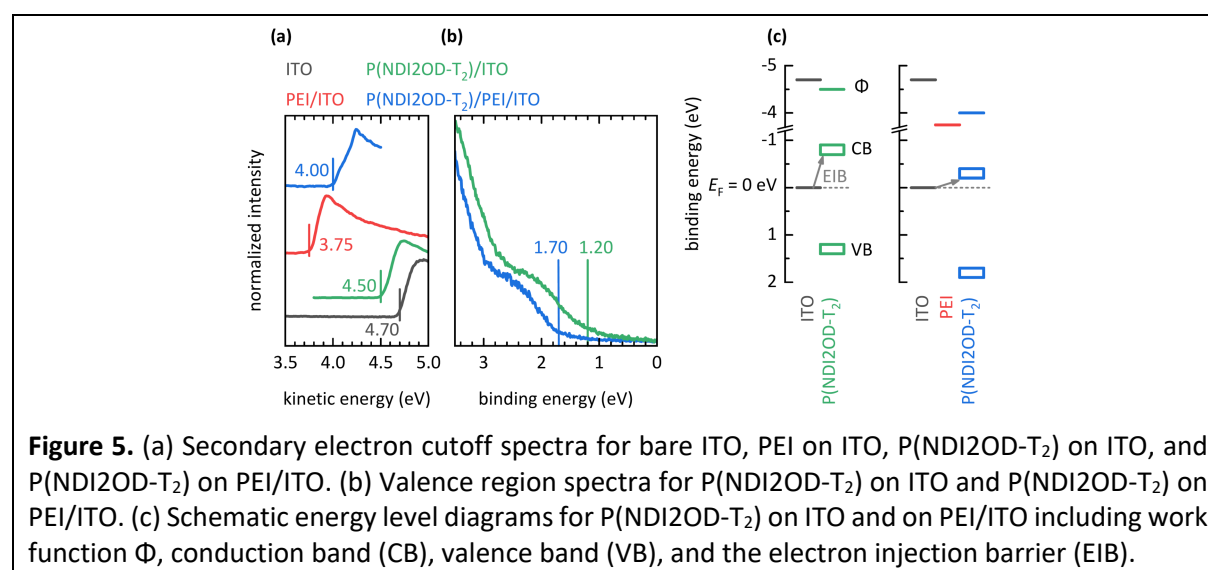
To demonstrate the accumulation of PEI at both the film top and bottom, we used X-ray photoelectron spectroscopy, for films prepared on ITO/glass. As inferred from the N 1s and S 2p core level spectra shown in Figure 4, the [S]:[N] atomic for the pure P(NDI2OD-T₂) film 1:1, which is in line with the chemical structure of the polymer. For a film made from solution blended with PEI (90%:10%) we find [S]:[N] being 1:3, i.e., a much higher fraction of nitrogen is present at the surface. Here, the nitrogen core level has two components. From comparison with the spectrum obtained for the pure P(NDI2OD-T₂) film, we can assign the peak at higher binding energy to nitrogen in the imide groups of the P(NDI2OD-T₂) and the peak at lower binding energy to the nitrogen in the amine group of the PEI. Notably, the amount of nitrogen from PEI is much higher than expected for a homogeneous distribution of both polymers in the mixed film, for the given concentration ratio in solution. This indeed provides evidence for accumulation of PEI at the film surface, as suggested above from a morphology point of view. Next, we removed the mixed polymer film by peeling with adhesive tape. After this procedure, the intensity of the S 2p core level is strongly decreased, while the N 1s signal is

still comparably high (topmost spectra in Fig 4); we find [S]:[N] being 1:41, i.e., predominantly P(NDI2OD-T₂) is removed. The binding energy of the major N 1s component after peeling fits to that of the amine group, which also provides evidence for the accumulation of PEI at the film bottom. From both, scanning force microscopy and X-ray photoelectron spectroscopy results, we conclude that vertical phase separation in thin films made from P(NDI2OD-T₂):PEI solutions occurs, where the semiconductor is sandwiched between a top and a bottom PEI-rich layer.



Knowing with confidence that PEI dominates the contact to ITO in mixed films, we can use sequential deposition of the two polymers to investigate the energy level alignment at the interface with ultraviolet photoelectron spectroscopy, i.e., how electron injection is modified by the presence of PEI and the expected lowering of the work function. Photoelectron spectra recorded for the secondary electron cutoff for bare ITO, pure P(NDI2OD-T₂) on ITO, PEI on ITO, and P(NDI2OD-T₂) on PEI/ITO are

displayed in Figure 5a. The work function of ITO is 4.70 eV and is reduced to 4.50 eV upon deposition of pure P(NDI2OD-T₂) due to the push-back effect.[25] A thin layer of PEI (ca. 5 nm) on ITO reduces the work function to 3.75 eV, comparable to previously reported values.[1] The deposition of P(NDI2OD-T₂) on PEI/ITO leads to an increase of the work function to 4.00 eV. The valence region of P(NDI2OD-T₂) is shown in Figure 5b, without and with PEI layer on ITO. The valence band onset of pure P(NDI2OD-T₂) is 1.2 eV below the Fermi level, and it is 1.70 eV below the Fermi level with the PEI interlayer. The latter is the same value as found for P(NDI2OD-T₂) deposited on a CaO_x electrode, which had an even lower work function than PEI-covered ITO.[26] For both samples we find the same ionization energy (5.70 eV) for P(NDI2OD-T₂).[26] The work function increase upon depositing P(NDI2OD-T₂) on PEI/ITO can be readily explained by Fermi level pinning at the conduction band of the semiconductor polymer [27] If the substrate work function is lower than the electron affinity of the polymer, electron transfer to the polymer affinity level occurs to establish electronic equilibrium, and this interfacial charge rearrangement increases the work function. The situation is summarized in the schematic energy level diagrams shown in Figure 5c. Since empty levels, such as the conduction band, cannot be detected with direct photoelectron spectroscopy, we use a common approximation. Taking the optical gap of 1.50 eV of P(NDI2OD-T₂) in films (as shown in Figure 6), and adding a typical value of the exciton binding energy of conjugated polymers (0.4 eV), results in an estimated transport gap of 1.90 eV for P(NDI2OD-T₂). With the valence band onset at 1.70 eV below the Fermi level, the conduction band onset is placed 0.20 eV above the Fermi level. This position is in line with what was found earlier for P(NDI2OD-T₂) films on substrates with a work function up to 4.15 eV, where Fermi level pinning still occurs.[28]



The conduction band Fermi level pinning described above results in a significantly reduced electron injection barrier (EIB) for P(NDI2OD-T₂) films, from 0.70 eV on bare ITO to only 0.20 eV on PEI/ITO (see Figure 5c). An analogous EIB reduction is thus also expected for films deposited from blended P(NDI2OD-T₂):PEI solution, due to the vertical phase separation discussed further above.

While the reduced EIB can explain the reduced contact resistance upon adding PEI to P(NDI2OD-T₂) solutions, it does not relate to the higher polymer film conductivity. Thus we turn towards investigating to what extent the semiconducting polymer can be doped by PEI, since despite the pronounced vertical phase separation some of the PEI may well be present within the P(NDI2OD-T₂) phase. Absorption measurements were performed to check for typical signatures of charge transfer and polaron formation, in solution and films (Figure 6). Both P(NDI2OD-T₂) solution and film show an absorption onset at ca. 1.50 eV and absorption maxima at ca. 1.75 eV ca. 3.15 eV, as reported before. [22,29] Notably, no obvious changes upon blending PEI into P(NDI2OD-T₂) are observed, neither in solution

nor in thin films. In literature, blending P(NDI2OD-T₂) with tetrakis(dimethylamino)ethylene and in spectroelectrochemistry, both leading to charge transfer, was shown to give rise to additional absorption features below the original absorption onset and in between the two absorption peaks of neutral P(NDI2OD-T₂).[22,29] If doping occurred in our samples, the density of doping-induced polarons is below the detection limit of standard absorption spectroscopy.

For completeness, we mention that hydrogen release from the polymer may be a possibility to create charges on the polymer chain. Therefore, absorption measurements were performed for P(NDI2OD-T₂) blended with tetrabutylammonium hydroxide in solution (not shown); no changes in the absorption compare to pure P(NDI2OD-T₂) were observed.

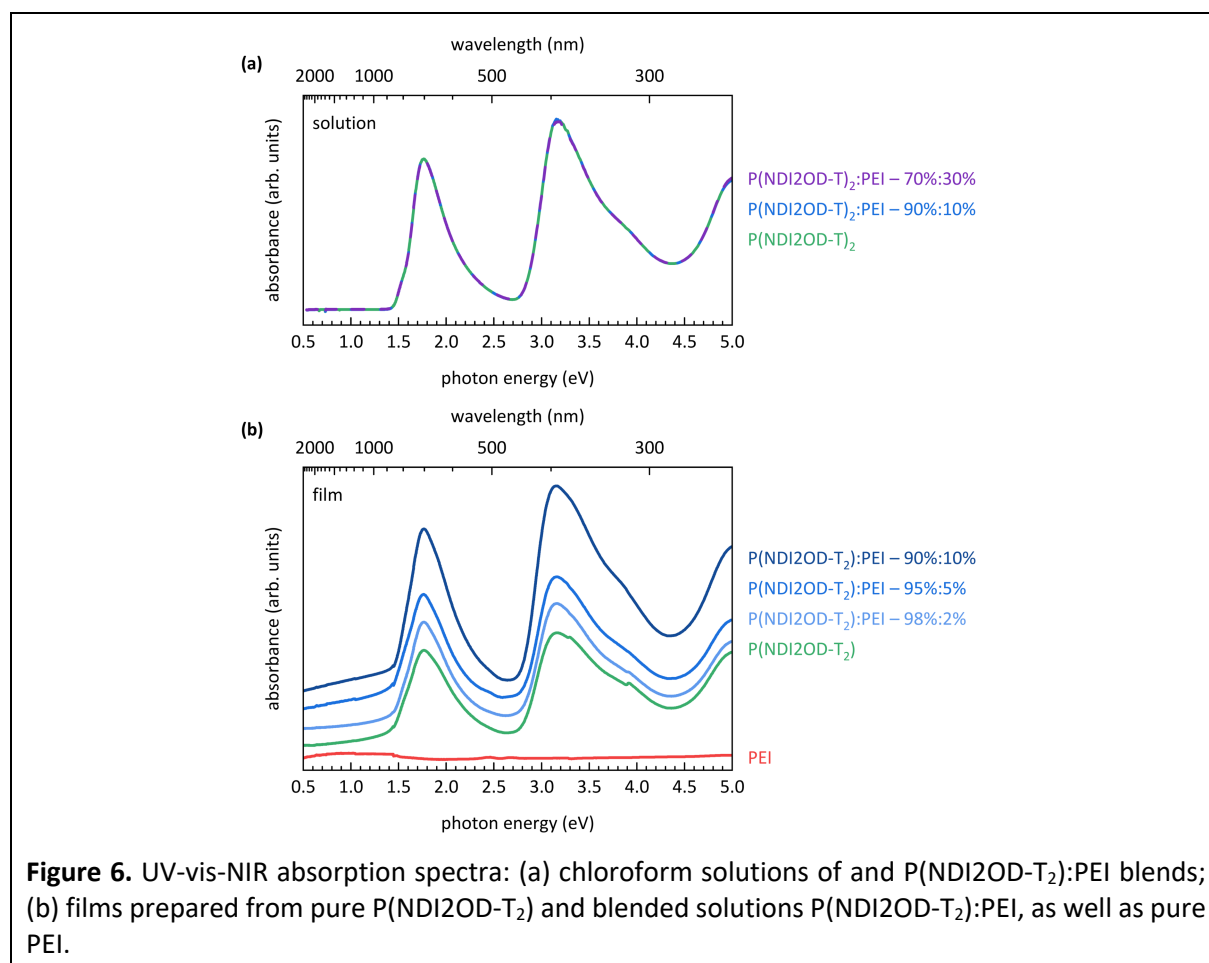
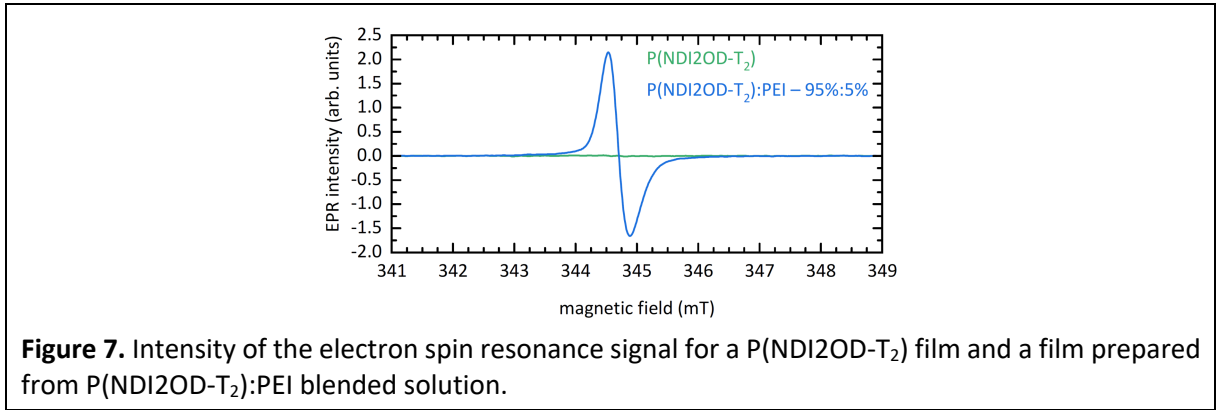


Figure 6. UV-vis-NIR absorption spectra: (a) chloroform solutions of and P(NDI2OD-T₂):PEI blends; (b) films prepared from pure P(NDI2OD-T₂) and blended solutions P(NDI2OD-T₂):PEI, as well as pure PEI.

A method with higher sensitivity with respect to charge carriers (with unpaired spin) is quantitative EPR, which we thus applied. The measured first-derivative EPR spectra for a P(NDI2OD-T₂) film and a film prepared from P(NDI2OD-T₂):PEI (95%:5%) solution are shown in Figure 7. While the spectrum of the P(NDI2OD-T₂) film does not show a significant signal, but an appreciable signal was measured for the film made from P(NDI2OD-T₂):PEI solution. Double integration and background correction gives $(1.2 \pm 0.3) \times 10^{-5}$ spins per polymer repeating unit (spin density $\approx 8 \times 10^{15} \text{ cm}^{-3}$) for the pure P(NDI2OD-T₂) film and $(8 \pm 2) \times 10^{-4}$ spins per repeating unit of P(NDI2OD-T₂) in the film blended with PEI (spin density $\approx 6 \times 10^{17} \text{ cm}^{-3}$). The spin density is thus increased by a factor of about 70 due to addition of 5% PEI. The sign of charges could not be determined with EPR, and it remains elusive whether electrons or holes were detected. Yet, it appears reasonable to assume an increased electron density in P(NDI2OD-T₂) upon adding PEI, and thus conclude that a very low-level doping and concomitant carrier

density increase takes place in solid blended films. It should also be mentioned that for solutions of pure and blended P(NDI2OD-T₂) we did not find an increases in spin density upon PEI addition.



So far, we unraveled that vertical phase separation in thin films prepared from blended P(NDI2OD-T₂):PEI solution leads to the predominant semiconductor phase being sandwiched between predominant PEI phases. The PEI accumulation at the ITO contact significantly reduces the electron injection barrier and thus the contact resistance. Low-level doping of P(NDI2OD-T₂) by PEI occurs, but it is not possible from EPR to conclude whether the detected spin density corresponds to indeed mobile carriers, or possibly immobile ones. If we assume that all detected electrons are mobile, then doping can contribute only approximately two orders-of-magnitude to the overall observed four orders-of-magnitude increase of the thin film conductivity σ upon PEI addition. However, if the electron density found for pure P(NDI2OD-T₂) corresponds to immobile carries only, the doping-induced electron density increase might account to the overall boost of conductivity upon addition of PEI.

Yet, since

$$\sigma = q \cdot n \cdot \mu(n) \quad (4)$$

where q is the unit charge, n the density of mobile charge carriers, and μ the n -dependent mobility [30–33], we discuss in the following possible causes for an increase of the apparent mobility by about two orders-of-magnitude. It is plausible that the vertical phase separation occurs not only on ITO but also on the bare glass (i.e., the channel in the two-terminal devices, in which the current flows). Residual hydroxyls on oxides, such as glass, can act as electron traps.[34] Due to vertical phase separation, a PEI layer separates the electron transporting P(NDI2OD-T₂) from the glass and its hydroxyls, thus reducing the detrimental effect of interfacial electron traps on n and μ , as suggested earlier.[17] However, this effect is limited to a very thin P(NDI2OD-T₂) layer in direct proximity of the glass substrate. Deep bulk electron traps are probably of minor relevance in P(NDI2OD-T₂) as trap-free space-charge limited current was reported in diodes.[35] Also, the electron affinity of P(NDI2OD-T₂) is lower than the trap energy related to water or oxygen in films.[36]. Variation of μ could be due to a slightly increased n , due to filling of shallow traps near the conductivity edge of the conduction band. [37] However, the density of detected charge carriers [$10^{-5} - 10^{-4}$ spins per P(NDI2OD-T₂) repeating unit, equivalent to a spin density in the range of ca. $10^{15} - 10^{17} \text{ cm}^{-3}$] is in a range where the n -dependence of μ is expected to have minor influence.[31,32] Improved polymer crystallinity, and thus mobility, was reported upon adding an insulating polymer to a semiconducting polymer.[38] However, given the pronounced top- and bottom phase separation observed here, and a lack of obvious morphology change upon PEI addition to P(NDI2OD-T₂) (Fig. 3), we do not consider this to be highly relevant for our samples. Finally, the morphology and crystallinity below the surface may be affected by the PEI layer, in comparison to a P(NDI2OD-T₂) film formed directly on glass [39]. This might result

in improved chain-ordering and thus higher μ , but detailed information on variations of crystallinity and chain-ordering with vertical resolution is not within reach of the present study.

Summary

We demonstrated that a self-organized low work function cathode interlayer of PEI forms on ITO upon spin coating a blended solution of P(NDI2OD-T₂) and PEI. Also, excess PEI is found at the surface of the polymer mixture, i.e., vertical phase separation results in a P(NDI2OD-T₂) rich phase sandwiched by PEI rich phases at the bottom and top of thin films. The bottom PEI layer is highly beneficial for electron injection into the semiconductor polymer, as the work function of PEI is sufficiently low to induce Fermi level pinning at the P(NDI2OD-T₂) conduction band, minimizing ohmic losses as the contact resistance is reduced by five orders of magnitude. Residual PEI within the P(NDI2OD-T₂) layer also dopes the semiconductor, however, at a very low level, that could not be detected by absorption spectroscopy, but only by more sensitive EPR measurements. Overall, the conductivity of mixed polymer films is up to four orders of magnitude higher than that of a pure P(NDI2OD-T₂) film. Plausibly, the low doping level fills electron traps close to the semiconductor conduction band, thus also increasing charge carrier mobility. The advantage of this one-step procedure to form PEI interlayers is obvious, but methods for improved control of residual PEI content in the semiconducting polymers should be identified, as even the low-level doping may not be advantageous for some applications.

Acknowledgments

The authors thank Timo Florian and Thorsten Schultz for help with electrical characterization and scanning force microscopy, respectively. We acknowledge support by the Deutsche Forschungsgemeinschaft (project numbers 286798544 and 182087777 - SFB 951). SRM acknowledges the Alexander von Humboldt Foundation for its generous support of a Senior Research Award to facilitate the collaborative activities described herein.

References

- [1] Y. Zhou, C. Fuentes-Hernandez, J. Shim, J. Meyer, A.J. Giordano, H. Li, P. Winget, T. Papadopoulos, H. Cheun, J. Kim, M. Fenoll, A. Dindar, W. Haske, E. Najafabadi, T.M. Khan, H. Sojoudi, S. Barlow, S. Graham, J.-L. Bredas, S.R. Marder, A. Kahn, B. Kippelen, A Universal Method to Produce Low-Work Function Electrodes for Organic Electronics, *Science* (80-.). 336 (2012) 327–332. <https://doi.org/10.1126/science.1218829>.
- [2] S. Fabiano, S. Braun, X. Liu, E. Weverberghs, P. Gerboux, M. Fahlman, M. Berggren, X. Crispin, Poly(ethylene imine) Impurities Induce n-doping Reaction in Organic (Semi)Conductors, *Adv. Mater.* 26 (2014) 6000–6006. <https://doi.org/10.1002/adma.201401986>.
- [3] M. Schneider, M. Brinkmann, H. Möhwald, Adsorption of Polyethylenimine on Graphite: An Atomic Force Microscopy Study, *Macromolecules*. 36 (2003) 9510–9518. <https://doi.org/10.1021/ma0345293>.
- [4] M. Fleischer, C. Schmuck, Transforming polyethylenimine into a pH-switchable hydrogel by additional supramolecular interactions, *Chem. Commun.* 50 (2014) 10464–10467. <https://doi.org/10.1039/C4CC03281K>.
- [5] S. Höfle, A. Schienle, M. Bruns, U. Lemmer, A. Colmann, Enhanced Electron Injection into Inverted Polymer Light-Emitting Diodes by Combined Solution-Processed Zinc Oxide/Polyethylenimine Interlayers, *Adv. Mater.* 26 (2014) 2750–2754. <https://doi.org/10.1002/adma.201304666>.
- [6] Z. Li, Y. Liang, Z. Zhong, J. Qian, G. Liang, K. Zhao, H. Shi, S. Zhong, Y. Yin, W. Tian, A low-work-function, high-conductivity PEDOT:PSS electrode for organic solar cells with a simple structure, *Synth. Met.* 210 (2015) 363–366. <https://doi.org/10.1016/j.synthmet.2015.11.006>.
- [7] P. Li, G. Wang, L. Cai, B. Ding, D. Zhou, Y. Hu, Y. Zhang, J. Xiang, K. Wan, L. Chen, K. Alameh, Q. Song,

- High-efficiency inverted polymer solar cells controlled by the thickness of polyethylenimine ethoxylated (PEIE) interfacial layers, *Phys. Chem. Chem. Phys.* 16 (2014) 23792–23799. <https://doi.org/10.1039/C4CP03484H>.
- [8] H. Kang, S. Hong, J. Lee, K. Lee, Electrostatically self-assembled nonconjugated polyelectrolytes as an ideal interfacial layer for inverted polymer solar cells, *Adv. Mater.* 24 (2012) 3005–3009. <https://doi.org/10.1002/adma.201200594>.
- [9] F.C. Wu, K.C. Tung, W.Y. Chou, F.C. Tang, H.L. Cheng, Charge selectivity in polymer:Fullerene-based organic solar cells with a chemically linked polyethylenimine interlayer, *Org. Electron.* 29 (2016) 120–126. <https://doi.org/10.1016/j.orgel.2015.11.037>.
- [10] Z. Li, F. Qin, T. Liu, R. Ge, W. Meng, J. Tong, S. Xiong, Y. Zhou, Optical properties and conductivity of PEDOT:PSS films treated by polyethylenimine solution for organic solar cells, *Org. Electron.* 21 (2015) 144–148. <https://doi.org/10.1016/j.orgel.2015.03.010>.
- [11] B.A.E. Courtright, S.A. Jenekhe, Polyethylenimine Interfacial Layers in Inverted Organic Photovoltaic Devices: Effects of Ethoxylation and Molecular Weight on Efficiency and Temporal Stability, *ACS Appl. Mater. Interfaces.* 7 (2015) 26167–26175. <https://doi.org/10.1021/acsami.5b08147>.
- [12] Y.H. Kim, T.H. Han, H. Cho, S.Y. Min, C.L. Lee, T.W. Lee, Polyethylene imine as an ideal interlayer for highly efficient inverted polymer light-emitting diodes, *Adv. Funct. Mater.* 24 (2014) 3808–3814. <https://doi.org/10.1002/adfm.201304163>.
- [13] S. Stolz, M. Scherer, E. Mankel, R. Lovrinčić, J. Schinke, W. Kowalsky, W. Jaegermann, U. Lemmer, N. Mechau, G. Hernandez-Sosa, Investigation of Solution-Processed Ultrathin Electron Injection Layers for Organic Light-Emitting Diodes, *ACS Appl. Mater. Interfaces.* 6 (2014) 6616–6622. <https://doi.org/10.1021/am500287y>.
- [14] S. Stolz, Y. Zhang, U. Lemmer, G. Hernandez-Sosa, H. Aziz, Degradation Mechanisms in Organic Light-Emitting Diodes with Polyethylenimine as a Solution-Processed Electron Injection Layer, *ACS Appl. Mater. Interfaces.* 9 (2017) 2776–2785. <https://doi.org/10.1021/acsami.6b15062>.
- [15] K.M. Kim, S. Ahn, W. Jang, S. Park, O.O. Park, D.H. Wang, Work function optimization of vacuum free top-electrode by PEDOT:PSS/PEI interaction for efficient semi-transparent perovskite solar cells, *Sol. Energy Mater. Sol. Cells.* 176 (2018) 435–440. <https://doi.org/10.1016/j.solmat.2017.11.002>.
- [16] S. Dong, Y. Wan, Y. Wang, Y. Yang, Y. Wang, X. Zhang, H. Cao, W. Qin, L. Yang, C. Yao, Z. Ge, S. Yin, Polyethylenimine as a dual functional additive for electron transporting layer in efficient solution processed planar heterojunction perovskite solar cells, *RSC Adv.* 6 (2016) 57793–57798. <https://doi.org/10.1039/C6RA09976A>.
- [17] D.X. Long, E.-Y. Choi, Y.-Y. Noh, High performance and stable naphthalene diimide based n-channel organic field-effect transistors by polyethylenimine doping, *Dye. Pigment.* 142 (2017) 323–329. <https://doi.org/10.1016/j.dyepig.2017.03.053>.
- [18] X. Zhang, C. Liu, Z. Li, J. Guo, Y. Zhou, L. Shen, L. Zhang, W. Guo, An easily prepared self-assembled interface layer upon active layer doping facilitates charge transfer in polymer solar cells, *Electrochim. Acta.* 285 (2018) 365–372. <https://doi.org/10.1016/j.electacta.2018.08.016>.
- [19] H. Kang, S. Kee, K. Yu, J. Lee, G. Kim, J. Kim, J.-R. Kim, J. Kong, K. Lee, Simplified Tandem Polymer Solar Cells with an Ideal Self-Organized Recombination Layer, *Adv. Mater.* 27 (2015) 1408–1413. <https://doi.org/10.1002/adma.201404765>.
- [20] S. Luan, G.W. Neudeck, An experimental study of the source/drain parasitic resistance effects in amorphous silicon thin film transistors, *J. Appl. Phys.* 72 (1992) 766–772. <https://doi.org/10.1063/1.351809>.
- [21] P. Pingel, M. Arvind, L. Kölln, R. Steyrlleuthner, F. Kraffert, J. Behrends, S. Janietz, D. Neher, P-Type Doping of Poly(3-hexylthiophene) with the Strong Lewis Acid Tris(pentafluorophenyl)borane, *Adv. Electron. Mater.* 2 (2016) 1–7. <https://doi.org/10.1002/aelm.201600204>.
- [22] S. Wang, H. Sun, U. Ail, M. Vagin, P.O.Å. Persson, J.W. Andreasen, W. Thiel, M. Berggren, X. Crispin, D. Fazzi, S. Fabiano, Thermoelectric properties of solution-processed n-doped ladder-type conducting polymers, *Adv. Mater.* 28 (2016) 10764–10771. <https://doi.org/10.1002/adma.201603731>.
- [23] G. Strobl, *The physics of polymers*, Springer Berlin Heidelberg, Berlin, Heidelberg, 2007. <https://doi.org/10.1007/978-3-540-68411-4>.
- [24] L. Qiu, J.A. Lim, X. Wang, W.H. Lee, M. Hwang, K. Cho, Versatile use of vertical-phase-separation-induced bilayer structures in organic thin-film transistors, *Adv. Mater.* 20 (2008) 1141–1145. <https://doi.org/10.1002/adma.200702505>.
- [25] M.T. Greiner, M.G. Helander, W.-M. Tang, Z.-B. Wang, J. Qiu, Z.-H. Lu, Universal energy-level alignment of molecules on metal oxides, *Nat. Mater.* 11 (2012) 76–81. <https://doi.org/10.1038/nmat3159>.
- [26] J. Frisch, A. Vollmer, N. Koch, Energy level pinning of an n-type semiconducting polymer on conductive

- polymer electrodes: Effects of work function and annealing, *J. Appl. Phys.* 112 (2012) 033712. <https://doi.org/10.1063/1.4745017>.
- [27] A. Crispin, X. Crispin, M. Fahlman, M. Berggren, W.R. Salaneck, Transition between energy level alignment regimes at a low band gap polymer-electrode interfaces, *Appl. Phys. Lett.* 89 (2006) 213503. <https://doi.org/10.1063/1.2396899>.
- [28] I. Lange, J.C. Blakesley, J. Frisch, A. Vollmer, N. Koch, D. Neher, Band Bending in Conjugated Polymer Layers, *Phys. Rev. Lett.* 106 (2011) 216402. <https://doi.org/10.1103/PhysRevLett.106.216402>.
- [29] D. Trefz, A. Ruff, R. Tkachov, M. Wieland, M. Goll, A. Kiriya, S. Ludwigs, Electrochemical investigations of the n-type semiconducting polymer P(NDI2OD-T2) and its monomer: new insights in the reduction behavior, *J. Phys. Chem. C* 119 (2015) 22760–22771. <https://doi.org/10.1021/acs.jpcc.5b05756>.
- [30] M.C.J.M. Vissenberg, M. Matters, Theory of the field-effect mobility in amorphous organic transistors, *Phys. Rev. B* 57 (1998) 12964–12967. <https://doi.org/10.1103/PhysRevB.57.12964>.
- [31] R. Coehoorn, W.F. Pasveer, P.A. Bobbert, M.A.J. Michels, Charge-carrier concentration dependence of the hopping mobility in organic materials with Gaussian disorder, *Phys. Rev. B* 72 (2005) 155206. <https://doi.org/10.1103/PhysRevB.72.155206>.
- [32] W.F. Pasveer, J. Cottaar, C. Tanase, R. Coehoorn, P.A. Bobbert, P.W.M. Blom, D.M. de Leeuw, M.A.J. Michels, Unified description of charge-carrier mobilities in disordered semiconducting polymers, *Phys. Rev. Lett.* 94 (2005) 206601. <https://doi.org/10.1103/PhysRevLett.94.206601>.
- [33] A. Salleo, Charge transport in polymeric transistors, *Mater. Today* 10 (2007) 38–45. [https://doi.org/10.1016/S1369-7021\(07\)70018-4](https://doi.org/10.1016/S1369-7021(07)70018-4).
- [34] L.-L. Chua, J. Zaumseil, J.-F. Chang, E.C.-W. Ou, P.K.-H. Ho, H. Sirringhaus, R.H. Friend, General observation of n-type field-effect behaviour in organic semiconductors, *Nature* 434 (2005) 194–199. <https://doi.org/10.1038/nature03376>.
- [35] H.T. Nicolai, M. Kuik, G.A.H. Wetzelaer, B. De Boer, C. Campbell, C. Risko, J.L. Brédas, P.W.M. Blom, Unification of trap-limited electron transport in semiconducting polymers, *Nat. Mater.* 11 (2012) 882–887. <https://doi.org/10.1038/nmat3384>.
- [36] D. Abbaszadeh, A. Kunz, N.B. Kotadiya, A. Mondal, D. Andrienko, J.J. Michels, G.-J.A.H. Wetzelaer, P.W.M. Blom, Electron Trapping in Conjugated Polymers, *Chem. Mater.* 31 (2019) 6380–6386. <https://doi.org/10.1021/acs.chemmater.9b01211>.
- [37] S. Olthof, S. Mehraeen, S.K. Mohapatra, S. Barlow, V. Coropceanu, J.-L. Brédas, S.R. Marder, A. Kahn, Ultralow Doping in Organic Semiconductors: Evidence of Trap Filling, *Phys. Rev. Lett.* 109 (2012) 176601. <https://doi.org/10.1103/PhysRevLett.109.176601>.
- [38] L. Qiu, W.H. Lee, X. Wang, J.S. Kim, J.A. Lim, D. Kwak, S. Lee, K. Cho, Organic Thin-film Transistors Based on Polythiophene Nanowires Embedded in Insulating Polymer, *Adv. Mater.* 21 (2009) 1349–1353. <https://doi.org/10.1002/adma.200802880>.
- [39] J. Veres, S. Ogier, G. Lloyd, D. de Leeuw, Gate Insulators in Organic Field-Effect Transistors, *Chem. Mater.* 16 (2004) 4543–4555. <https://doi.org/10.1021/cm049598q>.